Carbohydrate Polymers 75 (2009) 694–704

Contents lists available at ScienceDirect

Carbohydrate Polymers

journal homepage: www.elsevier.com/locate/carbpol

Starch vermicelli template-assisted synthesis of size/shape-controlled nanoparticles

Sanoe Chairam [a], Channarong Poolperm [b], Ekasith Somsook [b,*]

[a] Institute for Innovation and Development of Learning Process, Mahidol University, 272 Rama VI Road, Rachathewi, Bangkok 10400, Thailand
[b] NANOCAST Laboratory and Center for Alternative Energy, Department of Chemistry and Center of Excellence for Innovation in Chemistry, Faculty of Science, Mahidol University, 272 Rama VI Road, Rachathewi, Bangkok 10400, Thailand

ARTICLE INFO

Article history:
Received 6 August 2007
Received in revised form 12 August 2008
Accepted 12 September 2008
Available online 30 September 2008

Keywords:
Silver nanoparticles
Gold nanoparticles
Silver chloride nanoparticles
Starch
Green chemistry
Starch vermicelli

ABSTRACT

Size- and shape-controlled syntheses of silver and gold nanoparticles have been successfully developed using partially hydrolyzed starch vermicelli templates as green nanoreactors for the growth of nanoparticles. Mung bean vermicelli is of interest due to the higher amylose content and its transparency, allowing the formation of coloured particles on the vermicelli to be observed. The as-prepared silver and gold nanoparticles were characterized by UV–Visible spectroscopy, transmission electron microscopy (TEM), and X-ray diffraction (XRD). The carbonization of as-prepared vermicelli at 200 °C, 300 °C, and 500 °C was carried out to investigate nanoparticles embedded in the starch vermicelli templates. TEM of carbonized samples revealed the interesting patterns of gold nanorods and silver nanowire-liked assemblies along with carbon nanotubes. The carbonization of silver nanoparticles at 500 °C resulted to the loss of starch vermicelli capping nanoparticles and this led to the higher diffusion rate of nanoparticles to generate silver nanodendrites on TEM images. XRD data of carbonized yellow and purple silver nanoparticles revealed the presence of silver nanoparticles and a mixture of silver and silver chloride nanoparticles, respectively. This approach offers a great potential to design new fine structures of vermicelli and utilize its structure as a template for the large-scale synthesis of size- and shape-controlled silver and gold nanoparticles for chemical and biological applications.

1. Introduction

Inorganic nanoparticles have been attracting considerable interests due to their novel properties which are strongly influenced by size, shape, surface composition, spatial ordering, and interactions with surrounding environments (Cushing, Kolesnichenko & O'Connor, 2004; Daniel & Astruc, 2004; He, Kunitake, & Nakao, 2003; Panigrahi et al., 2006; Qu, Dai, & Osawa, 2006; Sun & Xia, 2002). The development has been focused on the inorganic nanostructures attached on the surface and embedded in the biomolecular structures such as DNA (Dean, Haynes, & Schmaljohn, 2005; Hill, Lyon, Allen, Stevenson, & Shear, 2005; Stoeva, Lee, Thaxton, & Mirkin, 2006; Xu, Hua Zeng, Lu, & Bing Yu, 2006), polypeptides (Chumbimuni-Torres et al., 2006; Xu et al., 2006), and virus (Deniger, Kolokoltsov, Moore, Albrecht, & Davey, 2006) for many applications in nanoelectronics, drug delivery, and catalysis. Among several biomolecules, starch is one of the most abundant materials on earth. The knowledge on the structure of starch has been recently advanced (Gidley, 2001). The description of starch is well-known as polymer structures containing mostly linear amylose and branched amylopectin. The spectroscopic and microscopic methods are now well advanced for probing the branching pattern and the branch length of starch polymers (Baker, Miles, & Helbert, 2001; Gallant, Bouchet, & Baldwin, 1997; Gidley, 1985; Jodelet, Rigby, & Colquhoun, 1998). The structure of starch is packed in semicrystalline granules containing concentric growth rings. Amylose and amylopectin are arranged radically and aligned perpendicularly to the growth rings and to the granule surface. Starch granules can be transformed into other forms such as starch paste, starch gel, and retrograded starch depending on the cooking conditions (Buléon, Colonna, Planchot, & Ball, 1998; Jenkins & Donald, 1995; Moorthy, Andersson, Eliasson, Santacruz, & Ruales, 2006; Rindlav-Westling, Stading, & Gatenholm, 2002; Tester, Karkalas, & Qi, 2004). The starch transformation provides diverse structures and properties for numerous applications. For example, starch gels can be produced from high amylose mung bean starch which is a major material for producing transparent starch vermicelli (Oates, 1990; Tan, Gu, Zhou, Wu, & Xie, 2006).

Though it is cheap and widely-used, less attention has been paid to the construction of nanoarchitectures on the surface and embedded in the structure of starch. Several environmental friendly approaches have been shown by using starch and polysaccharides as templates for nanoparticles synthesis (Huang & Yang, 2004; Lu, Gao, & Komarneni, 2005; Raveendran, Fu, & Wallen, 2003; Raveendran, Fu, & Wallen, 2006; Sarma & Chattopadhyay, 2004). The concept of green chemistry used in the synthesis of nanoparticles was first reported by Wallen and co-workers in

* Corresponding author. Tel.: +662 201 5123; fax: +662 354 7151.
E-mail address: scess@mahidol.ac.th (E. Somsook).

0144-8617/$ - see front matter © 2008 Elsevier Ltd. All rights reserved.
doi:10.1016/j.carbpol.2008.09.022

which the synthesis of silver nanoparticles was carried out and stabilized by soluble starch and using β-D-glucose as a nontoxic reducing agent (Raveendran et al., 2003; 2006). In the past decade, starch has been shown as a good host for many guests of inorganic nanoparticles, such as gold (Daniel & Astruc, 2004), silver (Raveendran et al., 2003) and iron oxides (Chairam & Somsook, 2008; Somsook et al., 2005) to form inclusion complexes. In this study mung bean vermicelli is of interest due to the higher amylose content and its transparency, allowing the formation of coloured particles on the vermicelli to be observed. Furthermore, it would be interesting if amylose or amylopectin containing glucose units could be utilized as a template for the fabrication of nanoparticles for potential applications in chemistry and biology. Here we demonstrated a simple fabrication of size- and shape-controlled silver and gold nanoparticles on the surface and embedded in the mung bean starch vermicelli.

2. Experimental

2.1. Materials and equipments

All materials in our experiments are biocompatible and environmental-friendly. Silver nitrate ($AgNO_3$) and hydrogen tetrachloroaurate(III) trihydrate ($HAuCl_4{\cdot}3H_2O$, ⩾99.9+%) were purchased from VWR international Ltd. and Sigma–Aldrich, respectively. β-D-glucose was purchased from Ajax Finechem. Hydrochloric acid (HCl), 98% AR grade, was purchased from Merck. Mung bean starch vermicelli, "Kaset" and "Dragon" brands (Bangkok, Thailand), was purchased from local supermarkets. All glassware used in this experiment was cleaned with an aqueous 10% nitric acid solution, washed with de-ionized water obtained from a Nanopure® Analytical Deionization system with an electric resistance 18.2 MΩ-cm purified with a Barnstead Nanopure Ultrapure Water system, and dried before use. A microwave machine used was M181 GN Samsung household microwave with an operating power output from 100–850 W, 7 power levels, and 35 min dual-speed timer.

2.2. Conventional heating

In a typical condition, 5 mL of 0.1 M solution of $AgNO_3$ or 0.1% of $HAuCl_4{\cdot}3H_2O$ was added to 300 mL of distilled water with 0.51 g of mung bean starch vermicelli under argon gas. The pH of the reaction was adjusted to a pH of 4 by diluted HCl in order to partially hydrolyze the surface of mung bean starch vermicelli. The reaction mixture was stirred for 1 h under argon gas, then 7.5 mL of 0.1 M of β-D-glucose was added and the reaction was continually stirred for 20 h. Mung bean starch vermicelli pieces were then collected from the reaction, dried in an oven at 60 °C prior to further analysis.

2.3. Microwave heating

A typical synthesis of nanoparticles with microwave heating was carried out as follows. First, 0.50 g of mung bean starch vermicelli was added to a 50 mL of deionized water and then heated in a microwave oven for 1 min to soak starch vermicelli in water. Then 150 μL of metal salt solution and 300 μL of 0.1 M of β-D-glucose were added to the reaction and heated in a microwave for a given period. The lowest power of the microwave oven at 100 W was chosen. Mung bean starch vermicelli pieces were then collected from the reaction, dried in an oven at 60 °C prior to further analysis.

2.4. Carbonization of vermicelli

Vermicelli with nanoparticles was heated in a crucible in a furnace at 200 °C, 300 °C and 500 °C in an ambient atmosphere for 48 h, respectively. A black precipitate was then obtained and dispersed in water by sonication in an ultrasonic bath for a given period.

2.5. The origin colours of purple and yellow silver nanoparticles

To further investigate the origin of two colours of vermicelli, two separated experiments were carried out and then followed by the carbonization.

2.5.1. Synthesis of yellow vermicelli

About 50 mL of deionized water was added into 0.5 g of mung bean starch vermicelli in a 250 mL beaker. Then, 5 mL of 0.1 M of $AgNO_3$ was added into the beaker. The reaction solution was heated by a microwave oven at 100 W in the presence of air for 5 min. After that, the mixture was transferred into a 100 mL Schlenk flask. A 7.5 mL of 0.1 M of β-D-glucose was added into the reaction flask. The reaction was heated at 60 °C and stirred under argon gas for 6 h. The colour of vermicelli was observed with a yellow colour. The mixture solution was cooled to room temperature. Mung bean starch vermicelli pieces were then collected from the reaction, dried in an oven at 60 °C prior to further analysis.

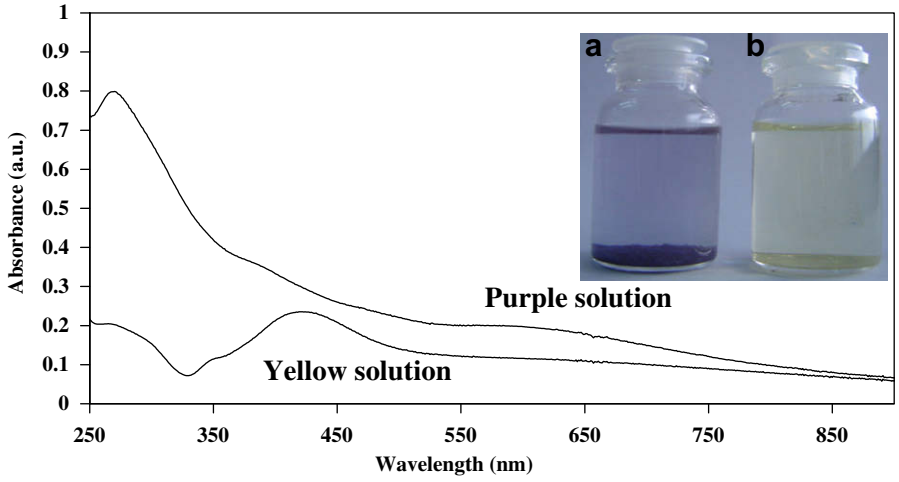

Fig. 1. UV–Visible spectra of purple and yellow colloidal solutions. The inset picture is purple (a) and yellow solutions (b) after removing vermicelli and centrifugation, respectively.

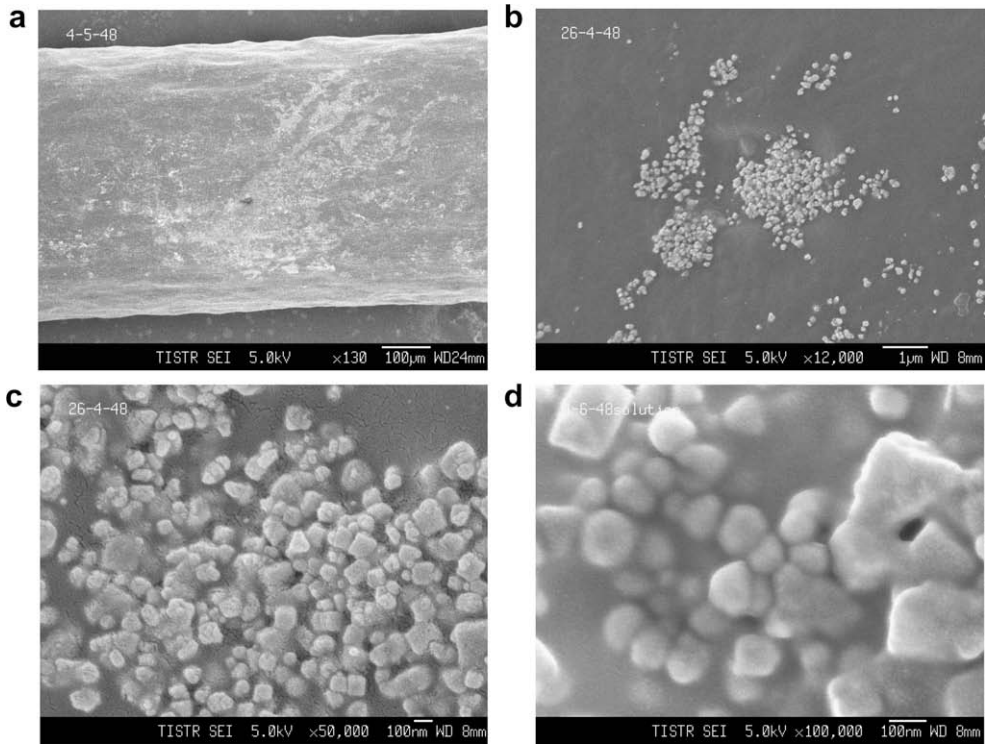

Fig. 2. FESEM of silver nanoparticles on the surface of mung bean starch vermicelli in different views and magnification powers. The bars for (a–d) are 100 μm, 1 μm, 100 nm, and 100 nm, respectively.

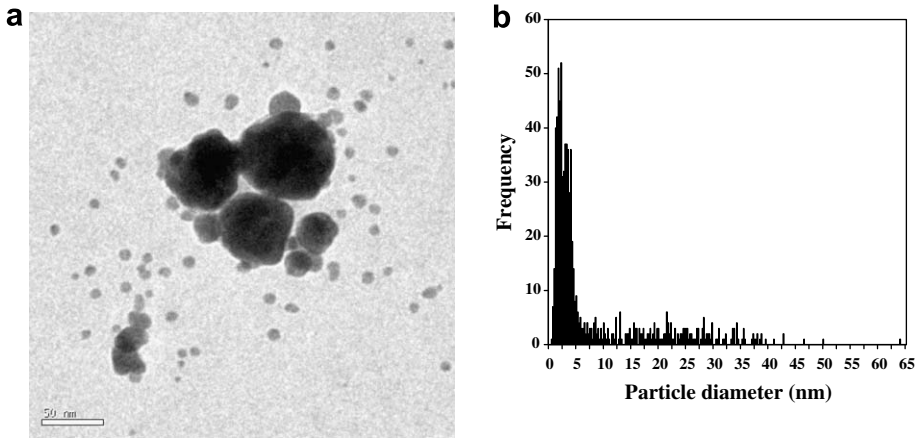

Fig. 3. (a) TEM image of starch silver nanoparticles in colloidal solution. The bar is 50 nm. (b) Histogram showing the size distribution of purple silver nanoparticles on the surface of vermicelli and in colloidal solution. The total number of counted nanoparticles is 806.

Fig. 4. Photographs of vials containing: (a) only starch vermicelli without the reduction of gold nanoparticles (left) and starch vermicelli capped gold nanoparticles (right): (b) and (c) starch vermicelli capped gold nanoparticles after the period time of three days and three months of storage at room temperature, respectively.

2.5.2. Synthesis of purple vermicelli

About 50 mL of deionized water was added into 0.5 g of mung bean starch vermicelli in a 250 mL beaker. After that, 5 mL of 0.1 M of $AgNO_3$ was added into the beaker. The reaction solution was heated by a microwave oven at 100 W in the presence of air for 5 min. The vermicelli was then washed with a dilute solution of NaCl. The mixture was transferred into a 100 mL Schlenk flask. 7.5 mL of 0.1 M of β-D-glucose was added into the reaction flask. The reaction was heated at 60 °C and stirred under argon gas for 6 h. The colour of vermicelli was observed with a purple colour. Then, the mixture solution was cooled to room temperature. Mung bean starch vermicelli pieces were then collected from the reaction, dried in an oven at 60 °C prior to further analysis.

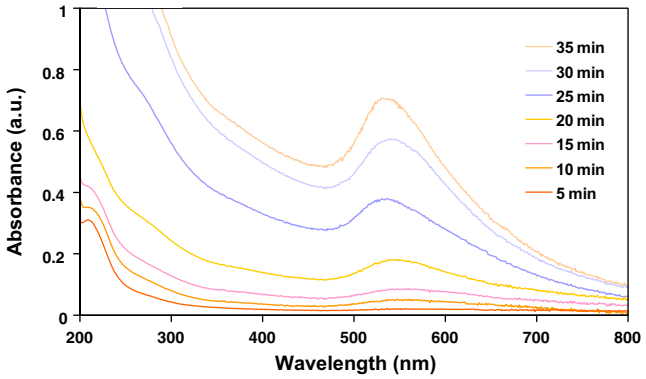

Fig. 5. UV–Visible absorption spectra showing the time evolution of the growth of gold nanoparticles at the different reaction time from 5 to 35 min.

2.5.3. Carbonization of vermicelli

As-prepared vermicelli with silver nanoparticles was heated in an alumina cup in a furnace at 200 °C and 300 °C in the ambient atmosphere for 24 h. Samples were placed in an alumina cup and heated at a heating rate of 5 °C min^{-1}. A black precipitate was obtained and characterized by XRD.

2.6. Characterization

The morphologies of nanostructures were recorded using a JEOL JSM-6340 F field emission scanning electron microscope (FESEM) with energy dispersive X-ray analysis (EDX). The XRD was carried out on a D8 Advance Bruker analytical X-ray system operating at the CuK_α wavelength of 1.5650 nm, 40 mA, and 40 kV. The diffraction patterns over the range of 30–70 ° of 2θ were recorded at a scan rate of 5 s/step and step size 0.020 2θ/s. The TEM micrographs of the as-synthesized samples were performed with a Philip Tecnia-G2 Sphera Transmission Electron Microscope by accelerating voltage at 80 kV. The UV absorption spectra of colloidal metal nanoparticles were performed by using a HP8453 HEWLETT PACKARD UV–Visible spectrophotometer with the path length of the quartz cell at 10 mm, over the wavelength ranging from 250 to 900 nm.

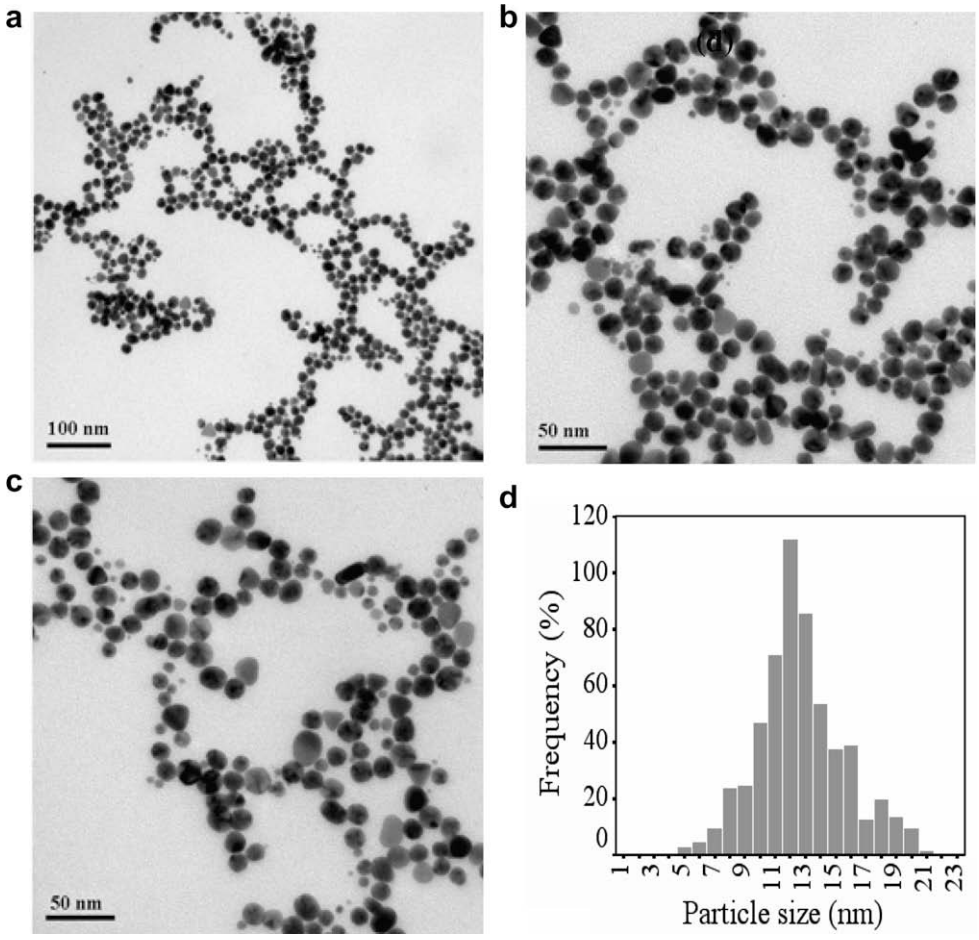

Fig. 6. TEM images of as-synthesized gold nanoparticles corresponding to a histogram of the size distribution from TEM micrographs (average particle size = 12.7 ± 2.8 nm). The bars of (a–c) are 100, 50 and 50 nm, respectively. The total number of single particles counted for a histogram is 573.

3. Results and discussion

3.1. Synthesis of silver nanoparticles

Following conventional heating of the reaction mixture for 2–3 h, a purple colour was observed for the mung bean starch vermicelli and the solution also adopted a purple colour which increased in intensity with time. Fragments of starch were detached from the vermicelli to generate a colourful purple solution. After the purple colloidal solution was centrifuged, the colour of the colloidal solution turned to yellow. The particle growth was monitored using UV–Visible absorption spectroscopy in which the strong, medium and weak absorption bands were observed at 270, 390 and 600 nm, respectively. The UV–Visible spectra of purple and yellow solutions are shown in Fig. 1. The yellow solution exhibited the UV–Visible spectrum with λ_{max} at 420 nm which was similar to recently reported silver nanoparticles (Raveendran et al., 2003; 2006).

The typical FESEM images of silver nanoparticles attached to mung bean starch vermicelli are shown in Fig. 2. The average particle diameter of silver nanoparticles on the surface of mung bean starch vermicelli was approximately 20 nm. The biggest particle diameter on the surface was observed up to 65 nm. The TEM images of the purple suspension are also shown in Fig. 3a. It was unexpected that 40 nm range nanoparticles were found with 3 nm nanoparticles on the TEM images. The histogram of the size distribution of starch silver nanoparticles on the surface of vermicelli including those in colloidal solution displayed two different sizes of nanoparticles (1–5 nm and 10–65 nm) showing the broad particle size distribution (Fig. 3b). The smaller particles (Fig. 3b) were approximately the same particle size as Wallen's starch silver nanoparticles but the size distribution was narrower. The EDXspectrum confirmed the presence of silver, carbon, and oxygen as major elements suggesting that the interactions between silver and starch in the samples and silver nanoparticles must be stabilized by starch.

3.2. Synthesis of gold nanoparticles

Microwave heating speeds up the synthesis of nanoparticles. The colour of mung bean starch vermicelli turned to pale red after microwave irradiation for a couple of minutes (Fig. 4 and 5). Interestingly, starch vermicelli capped gold nanoparticles were stable in the vermicelli templates over the period time of three months of storage at room temperature, while there was no sign of aggregation of gold nanoparticles. This indicated that the mung bean starch vermicelli template could be used to prevent the aggregation of nanoparticles in sterile condition. The UV–Visible absorption spectra of colloidal gold solutions were collected to investigate the growth of nanoparticles by microwave irradiation at different reaction times (5–35 min). It was found clearly that the intensity of the surface plasmon band of colloidal gold nanoparticles increased with the reaction time. It is well-known that the colloidal gold nanoparticles in an aqueous solution exhibit a broad absorption band in the visible region at wavelength from 517 nm to 575 nm due to the Mie theory (Daniel & Astruc, 2004). As can be shown in Fig. 5, the results showed clearly that the strong absorption peaks of as-prepared gold nanoparticles showed

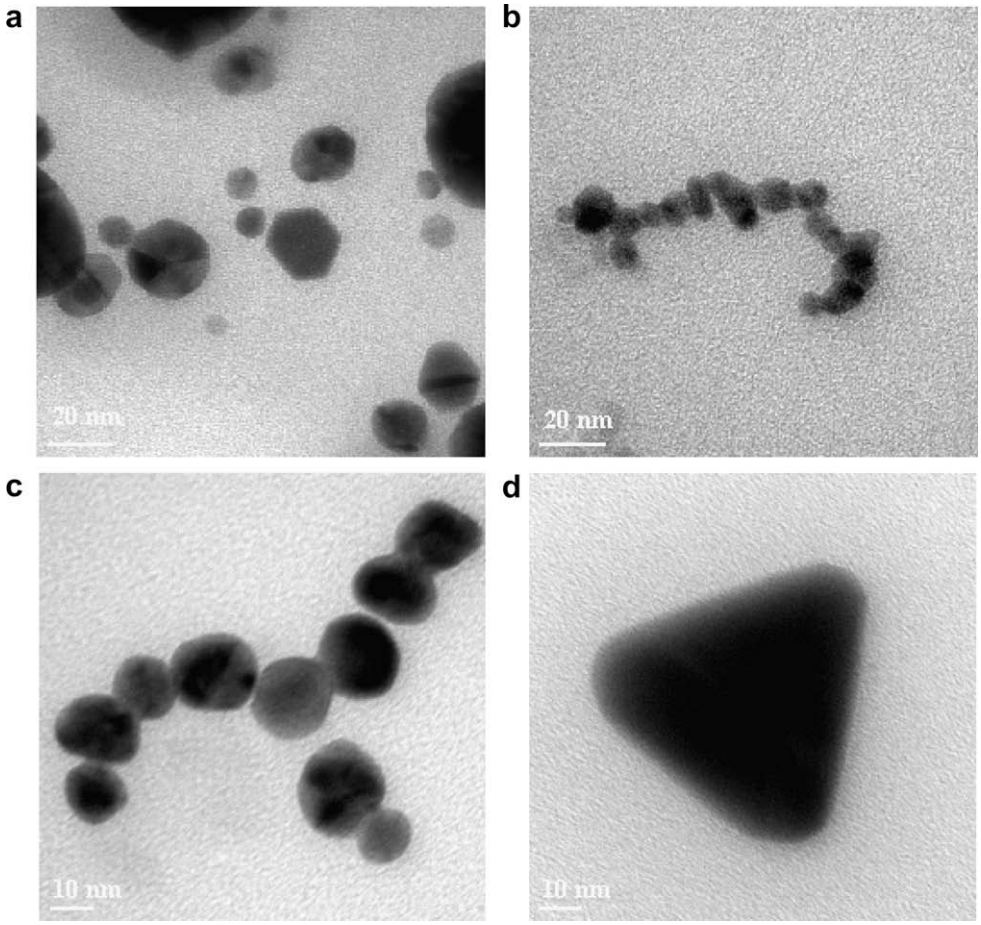

Fig. 7. HRTEM images of as-synthesized gold nanoparticles after microwave heating for 5 min. The bars of (a–d) correspond to 20, 20, 10, 10 nm, respectively.

a match with the reported results (Daniel & Astruc, 2004). These absorption values may not include the protecting agent of starch vermicelli templates, because the Mie scattering responds only to the nanoscale gold particles (Su et al., 2003; Templeton, Pietron, Murray, & Mulvaney, 2000). Also, the surface plasmon band was symmetric indicating that the colloidal solutions had no aggregation of particles. The strong intensity of an absorption peak became increasing indicating that the reduction reaction of gold nanoparticles had greatly proceeded. In addition, the tendency of the absorption peak also slightly shifted to blue, implying a decrease in the particle size for the formation of gold nanoparticles.

The morphologies and sizes of as-prepared gold nanoparticles were examined by TEM. As can be observed in Fig. 6, TEM images showed clearly well-dispersed gold nanoparticles synthesized at the different TEM magnifications corresponding to a histogram of the size distribution from TEM micrographs. The resulting product

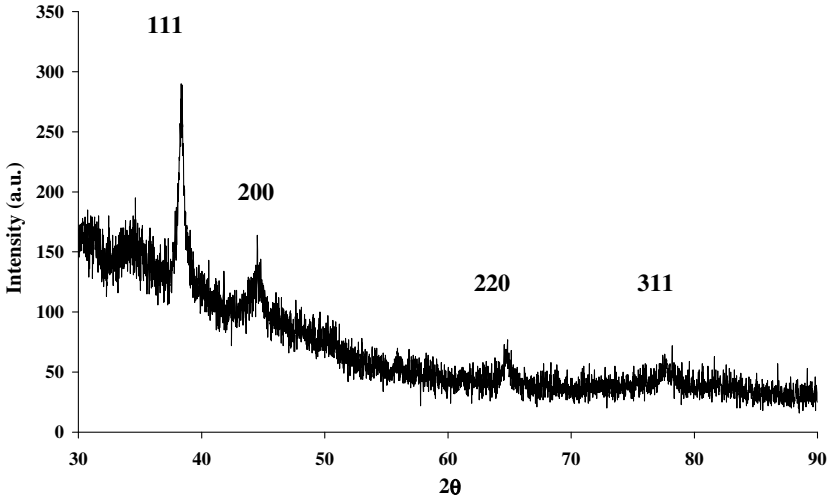

Fig. 8. The XRD pattern of the as-prepared gold nanoparticles.

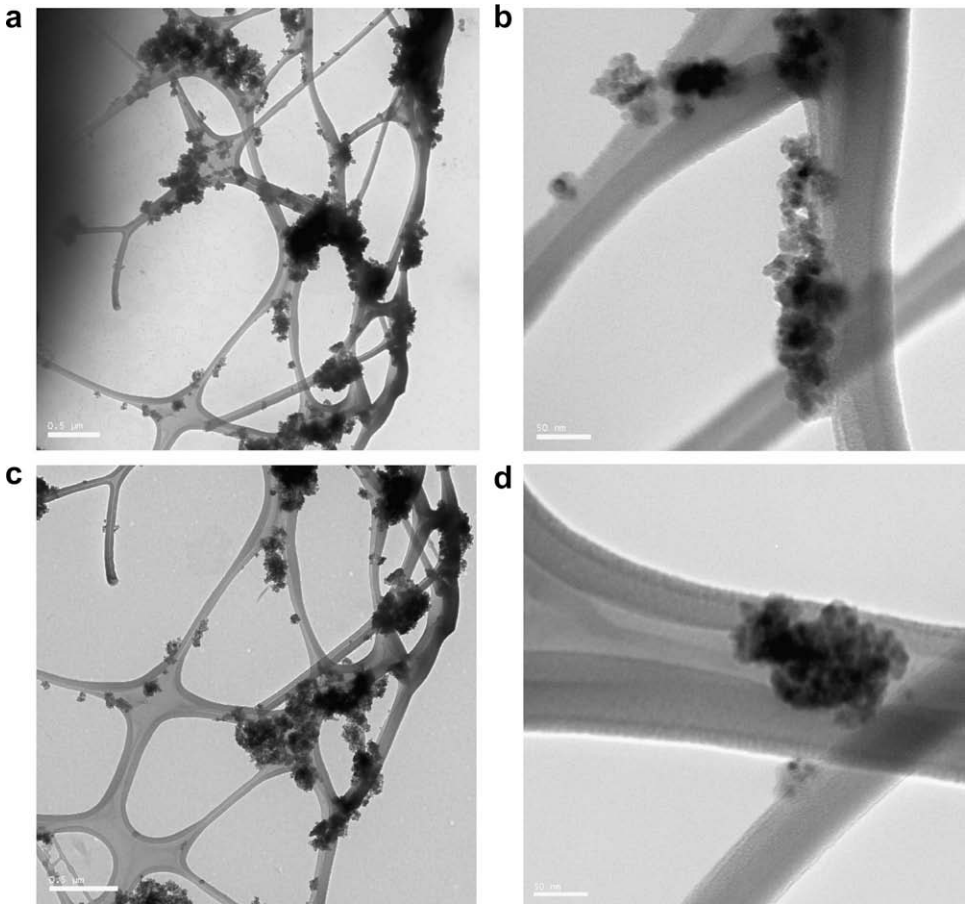

Fig. 9. TEM images of carbonization products at 200 °C with the sonication time of 30 min showing silver (a and b) and gold nanoparticles (c and d) attached to the surface of carbon nanotubes. The bars are 0.5 μm, 50 nm, 0.5 μm and 50 nm, respectively.

mainly consisted of an extremely uniform size of spherical gold nanostructures. The average particle size of the as-prepared gold nanoparticles with diameters was 12.7 nm with a standard deviation of 2.8 nm ($n = 573$), with a maximum of 21 nm in size distribution.

Interestingly, a few of different morphologies of the as-prepared gold nanoparticles were also found in the same sample. To obtain a clear picture, the regular structure of these particles was further examined using high-resolution TEM (HRTEM) observation. As shown in Fig. 7, a representative sample of the resulting product of various shapes (e.g., polygonal, hexagonal and triangular shape) of gold nanoparticles was obtained when increasing of the reaction time for the microwave heating process. As shown in Fig. 7b and c, gold nanowires with the approximate distance of 100 nm were observed in the same sample. It is suggested that the formation of nanowires jointed by gold nanoparticles was facilitated by the helical molecular structure of starch acting as nanoreactors.

In order to understand the crystalline structure of the gold nanoparticle formation, X-ray diffraction was carried out to investigate the atomic structure of small nanoparticles. It has been used as a common tool to examine the crystallinity of samples. After drying in an oven at 60 °C for 24 h, the dried powder product was ground and further characterized by XRD. The XRD pattern of the as-prepared gold nanoparticles is shown in Fig. 8. There were four diffraction peaks with the 2θ of 38.4, 44.5, 64.7 and 77.6 corresponding to the (111), (200), (220) and (311) planes, respectively, of the face-centered cubic (fcc) metallic gold (JCPDS file no.04-0784). These positions of the diffraction peaks of the as-prepared gold nanoparticles showed a match with the reported results (Lu et al., 2005). Since gold nanoparticles were embedded within mung bean starch vermicelli acting as stabilizing templates, the broad diffractions were observed over a 2θ range due to the low crystallinity of starch vermicelli.

3.3. Carbonization of nanoparticles embedded in vermicelli

The carbonization allows us to investigate the patterns of nanoparticles embedded in the starch vermicelli. First, vermicelli prepared by the microwave technique was carbonized in a crucible in an oven at 200 °C, 300 °C and 500 °C. After the carbonization, black vermicelli was obtained and then ground and dispersed in water by ultrasonic sonication. The 30 min duration time for the sonication was first chosen. TEM images of as-prepared samples are shown in Fig. 9. The aggregated nanoparticles were attached to carbon nanotubes which were confirmed by EDX spectra showing that the major elements of the carbon nanotubes were carbon and oxygen only. This is an alternative way to synthesize carbon nanotubes from saccharides.

Longer period of the sonication time led to the aggregation of the nanoparticles. Therefore, shorter period of the sonication time was carried out to disperse nanoparticles in water. TEM images of nanowire-like assemblies of silver nanoparticles and gold nanorods are shown in Fig. 10. The pattern of silver nanoparticles looks like to a wire in an electronic circuit even though nanoparticles were not totally next to each other. A histogram analysis showed that the mean particle diameter was observed at 8.24 nm with a standard deviation of 2.20 nm. This unique morphology is probably a result of the inclusion of silver nanoparticles in the amylose

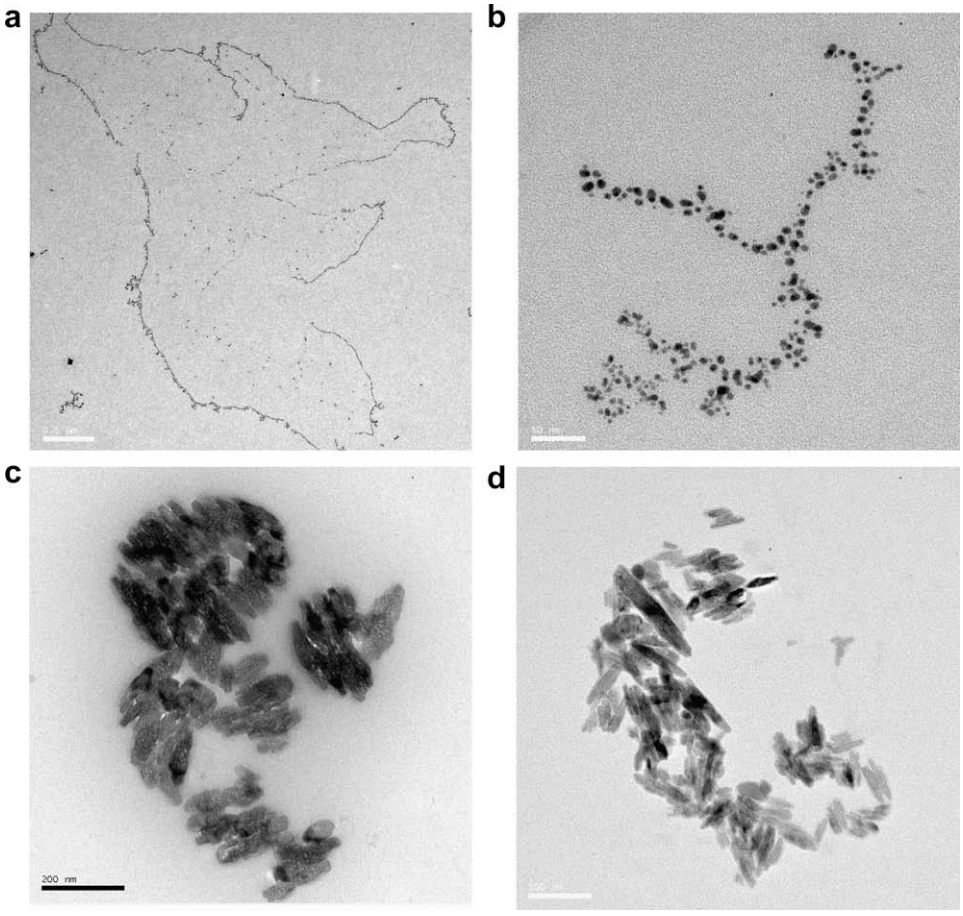

Fig. 10. TEM images of carbonization products at 200 °C (a–c) and 300 °C (d) with the sonication time of 10 min showing the self-assembly of silver nanowires (a and b) and gold nanorods (c and d). The bars are 0.5 μm, 50 nm, 200 nm, and 100 nm, respectively.

helical structure. Moreover, the particle size distribution of nanoparticles embedded in vermicelli was narrower than one in the colloidal solution. TEM images with low magnification clearly show lengthy gold nanorods with the lengths are up to 100 nm and the width is approximately 10–20 nm in which is about the same size of carbon nanotubes obtaining from the carbonization.

TEM images in Fig. 11 showed the growth of silver nanodendrites on a copper grid. This is well explained that the carbonization at higher temperature resulted the lower number of molecules of starch vermicelli capping nanopaticles. This led to the increasing diffuson rate resulting in the growth of nanodendrite of silver nanoparticles on copper grids. The average diameter of particles was 29.0 nm with a standard deviation of 10.54 nm. The growth mechanism of our nanodendrites is well described on the basis of a diffusion-limited aggregation (DLA) model (Kaniyankandy, Nuwad, Thinaharan, Dey, & Pillai, 2007) where the individual atoms are bond to the growing surface during the process.

3.4. Two colours of silver nanoparticles

To further investigate the origin of different colours of the as-prepared silver nanoparticles, two separate experiments were carried out by first incorporating Ag(I) ions into the inside of vermicelli by microwave radiation, then reducing Ag(I) ions to Ag(0) nanoparticles by β-D-glucose under an inert atmosphere with a conventional heating. The two experiments were different only in that the vermicelli for one experiment was washed with a solution of NaCl before heating with β-D-glucose. Two colours of silver nanoparticles were successfully synthesized (Fig. 12). Although the results from FESEM and TEM images demonstrated clearly that silver nanoparticles were produced on the surface of mung bean starch vermicelli and in the colloidal solution, the phase of silver nanoparticles was further examined by the carbonization of nanoparticles embedded in vermicelli at 200 °C and 300 °C and then characterized by XRD. After the carbonization of yellow (Fig. 12a) and purple (Fig. 12b) silver nanoparticles stabilized by

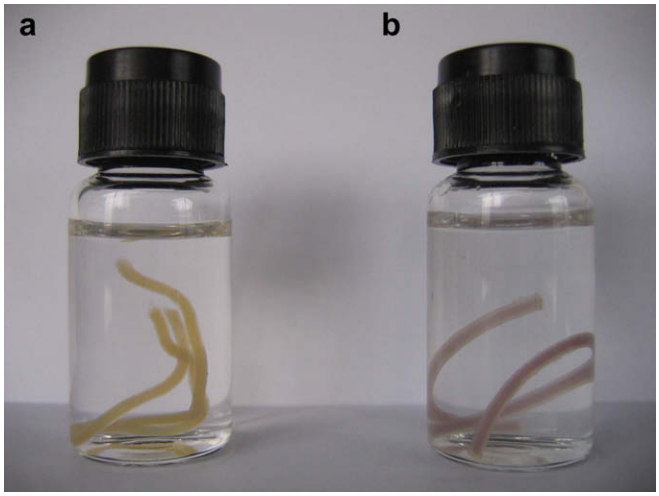

Fig. 12. Pictures of (a) yellow and (b) purple vermicelli fabricated with silver nanoparticles.

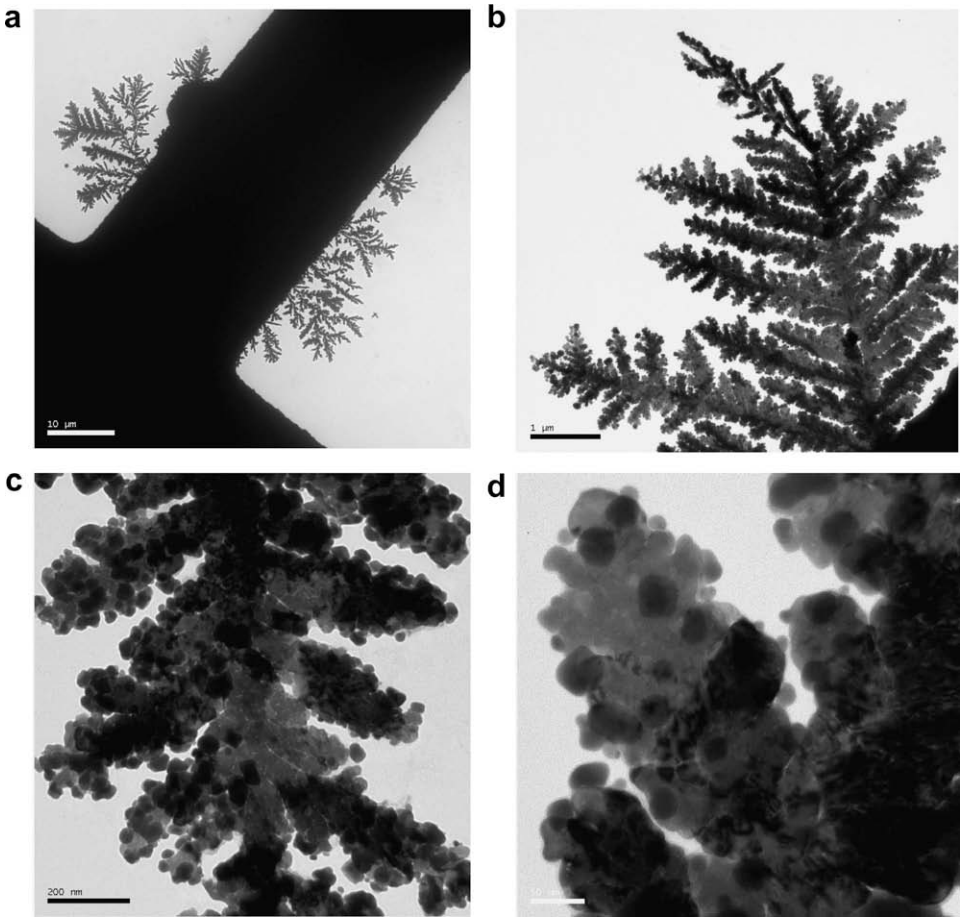

Fig. 11. (a–d) TEM micrographs of silver dendrites obtained from carbonization at 500 °C for 24 h. The bars are 10 μm, 1 μm, 200 nm and 50 nm, respectively.

vermicelli templates in a furnace at 200 °C and 300 °C for 24 h, a black precipitate powder was also obtained in a crucible cup. The XRD was used to examine the phase of the obtaining products. The diffraction patterns of two colours of yellow and purple vermicelli demonstrated different patterns (Fig. 13). From all diffraction patterns, the presence of metal oxides (e.g. silver oxide) was also not detected.

For the yellow mung bean starch vermicelli, the diffraction patterns (Fig. 6a and c) showed strong diffraction peaks assigned 2θ around 38.2°, 44.4° and 64.5°, which can be indexed to the (111), (200), and (220) planes of the face-centered cubic silver (JCPDS Card File, No. 04-0783). However, the diffraction pattern of yellow silver nanoparticles showed broad peaks on the diffractogram. This is possibly due to the inclusion of silver nanoparticles in the starch vermicelli templates. According to the molecular structure reported by Gidley (Gidley, 2001), it is now accepted that there is a continuum of starch polymer structures from linear amylose to branched amylopectin. This is suggested that the linear amylose- or branched amylopectin-nanoparticle complexes are formed to be non-crystalline in the native granule starch, indicating that the appearance of broad diffraction lines is present in a poor crystallinity for XRD patterns. The results obtained here were found to be similar to Sarma and Chattopadhyay (Sarma & Chattopadhyay, 2004) and Chairam and Somsook (Chairam & Somsook, 2008) who reported that a poor crystallinity was observed over a range of 2θ positions for starch-mediated synthesis of metal and metal-oxide nanoparticles, respectively. Therefore, some diffraction peaks were not observed from the XRD observation. After carbonization, it was noted that the absence of any different peaks was hidden most likely due to black carbon precipitate powder. The results from diffractogram indicated clearly that the origin of yellow vermicelli was demonstrated from the presence of silver nanoparticles.

Several 2θ positions of the diffraction pattern were observed for the sample obtaining from the carbonized purple vermicelli powder (Fig. 13b and d). In addition to the XRD pattern of Ag nanoparticles (peaks at 38.2°, 44.4°,and 64.6°), 5 other peaks are 32.3°, 46.4°, 54.9°, 57.6°, and 67.7° corresponding to the (200), (220), (311), (222), and (400) planes of the face-centered cubic AgCl (JCPDS Card File, No. 06-0480). The XRD indicated clearly the presence of silver chloride in the powder after the carbonization of purple vermicelli at 200 °C and 300 °C. AgCl nanoparticles have been reported as nanocomposites with other materials such as silk fibers (Potiyaraj, Kumlangdudsana, & Dubas, 2007) and polyaniline (Feng, Liu, Lu, Hou, & Zhu, 2006). Recently, Li and Zhu investigated the formation of Ag nanoparticles toward HCl. A white precipitate product was formed immediately when the HCl solution was added into a Ag colloidal solution (Li & Zhu, 2006). Li and Zhu also indicated that chloride ions could react with colloidal Ag nanoparticles; however, the purple silver nanoparticles were not reported. Interestingly, the purple silver nanoparticles were produced in our experiment. The vermicelli before and after washing with a diluted NaCl solution was still transparent. A white precipitate of silver chloride was not observed. After the reaction of silver ions with β-D-glucose using as a reducing agent, the colour of transparent vermicelli turned to purple. It might be possible that during the nanoparticles formation process some silver nanoparticles may react with chloride ions to form silver chloride. It is noted that all 2θ positions obtained from purple vermicelli were the combination of the diffraction patterns of silver chloride and silver nanoparticles. The nanoparticles in the range 10–65 nm in Fig. 3 are possibly silver chloride nanoparticles which could be separated out by centrifugation.

3.5. Utilization of the starch structure in the synthesis of nanoparticles

Starch has been used for the synthesis and stabilization of nanoparticles, such as gold and silver (Raveendran et al., 2003; 2006; Sarma & Chattopadhyay, 2004) due to its inexpensive and renewable with numerous applications. Starch is a polyhydroxylated macromolecules consisting of glucose units connected by an oxygen linkage to form amylose and amylopectin chains. It presents an interesting dynamic supramolecular associations facilitated by inter- and intra-molecular hydrogen bonding resulting helical structure, which can act as nanoreactors for the growth of nanoparticles (Imberty, Chanzy, Perez, Buleon, & Tran, 1988). During the microwave heating process, metal-aqua complexes were introduced into the starch vermicelli template. The hydroxyl groups of starch possibly facilitated metal ions by electrostatic binding in the helical structure of polysaccharide. Aldehyde terminals from the partial hydrolysis of starch reduced metal ions to metallic nanoparticles while mung bean starch vermicelli itself was used as templates to stabilize as-prepared nanoparticles (as shown in Scheme 1). It has been proposed that the nanoparticle size and polydispersity are controlled by the fine structure of protecting biomolecules including reducing reagents and thermodynamic conditions (Raveendran et al., 2003). Based on the model of starch structure (Buléon et al., 1998; Gallant et al., 1997; Jenkins & Donald, 1995; Tester et al., 2004), the formation of the 38 nm range silver nanoparticles was controlled by the size of helical amylose.

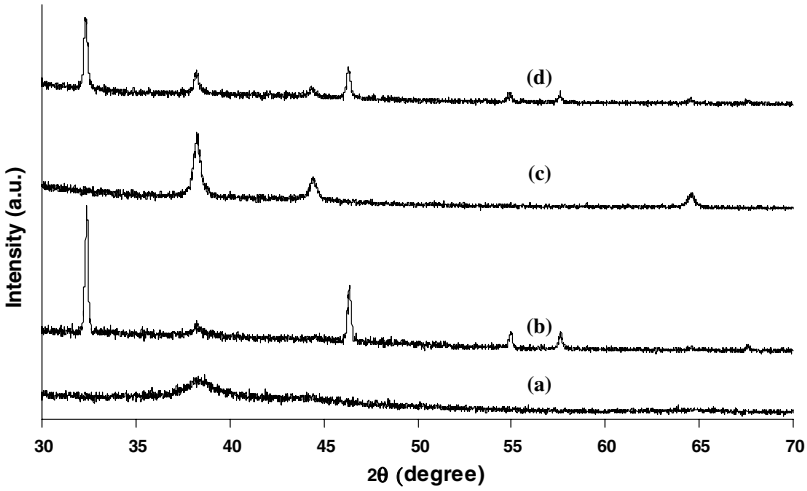

Fig. 13. XRD diffraction pattern of yellow vermicelli (a and c) and purple vermicelli (b and d) at 200 °C and 300 °C, respectively.

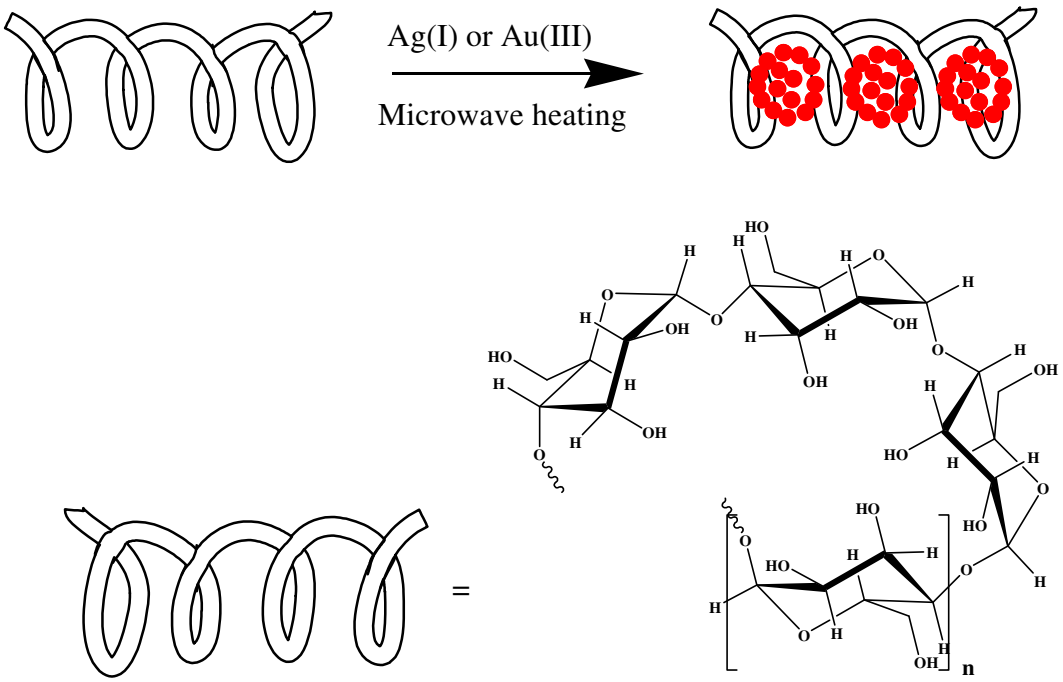

Scheme 1. Illustration of the helical structure of starch template-assisted synthesis of size-controlled nanoparticles.

4. Conclusion

In summary, we have successfully developed a green route to synthesize size- and shaped-controlled silver and gold nanoparticles using mung bean starch vermicelli acting as a stabilizing template. This approach to synthesize size- and shaped-controlled silver and gold nanoparticles is very simple, safe and easily accessible and offers an opportunity to design new fine structures and utilize mung bean starch vermicelli serving as raw materials for the large-scale synthesis of size- and shaped-controlled silver and gold nanoparticles for chemical and biological applications.

Acknowledgements

This research was supported by the Center for Innovation in Chemistry (PERCH-CIC), the Thailand Research Fund, The Commission on Higher Education (RMU4980050) and Faculty of Science, Mahidol University. We thank the Thailand Institute of Scientific and Technological Research (TISTR) for FESEM measurements.

References

Baker, A. A., Miles, M. J., & Helbert, W. (2001). Internal structure of the starch granule revealed by AFM. *Carbohydrate Research, 330*(2), 249–256.

Buléon, A., Colonna, P., Planchot, V., & Ball, S. (1998). Starch granules: structure and biosynthesis. *International Journal of Biological Macromolecules, 23*(2), 85–112.

Chairam, S., & Somsook, E. (2008). Starch vermicelli template for synthesis of magnetic iron oxide nanoclusters. *Journal of Magnetism and Magnetic Materials, 320*(15), 2039–2043.

Chumbimuni-Torres, K. Y., Dai, Z., Rubinova, N., Xiang, Y., Pretsch, E., Wang, J., & Bakker, E. (2006). Potentiometric biosensing of proteins with ultrasensitive ion-selective microelectrodes and nanoparticle labels. *Journal of the American Chemical Society, 128*(42), 13676–13677.

Cushing, B. L., Kolesnichenko, V. L., & O'Connor, C. J. (2004). Recent advances in the liquid-phase syntheses of inorganic nanoparticles. *Chemical Review, 104*(9), 3893–3946.

Daniel, M. C., & Astruc, D. (2004). Gold nanoparticles: assembly, supramolecular chemistry, quantum-size-related properties, and applications toward biology, catalysis, and nanotechnology. *Chemical Review, 104*(1), 293–346.

Dean, H. J., Haynes, J., & Schmaljohn, C. (2005). The role of particle-mediated DNA vaccines in biodefense preparedness. *Advanced Drug Delivery Reviews, 57*(9), 1315–1342.

Deniger, D. C., Kolokoltsov, A. A., Moore, A. C., Albrecht, T. B., & Davey, R. A. (2006). Targeting and penetration of virus receptor bearing cells by nanoparticles coated with envelope proteins of Moloney murine leukemia virus. *Nano Letters, 6*(11), 2414–2421.

Feng, X. O., Liu, Y. G., Lu, C. L., Hou, W. H., & Zhu, J. J. (2006). One-step synthesis of AgCl/polyaniline core-shell composites with enhanced electroactivity. *Nanotechnology, 17*(14), 3578–3583.

Gallant, D. J., Bouchet, B., & Baldwin, P. M. (1997). Microscopy of starch: evidence of a new level of granule organization. *Carbohydrate Polymers, 32*(3–4), 177–191.

Gidley, M. J. (1985). Quantification of the structural features of starch polysaccharides by NMR spectroscopy.. *Carbohydrate Research, 139*, 85–93.

Gidley, M. J. (2001). Starch structure/function relationships: achievements and challenges. In T. L. Barsby, A. M. Donald, & P. J. Frazier (Eds.), *Starch: advances in structure and function* (pp. 1–7). Cambridge, UK: The Royal Society of Chemistry.

He, J., Kunitake, T., & Nakao, A. (2003). Facile in-situ synthesis of noble metal nanoparticles in porous cellulose fibers. *Chemistry of Materials, 15*(23), 4401–4406.

Hill, R. T., Lyon, J. L., Allen, R., Stevenson, K. J., & Shear, J. B. (2005). Microfabrication of three-dimensional bioelectronic architectures. *Journal of the American Chemical Society, 127*(30), 10707–10711.

Huang, H., & Yang, X. (2004). Synthesis of polysaccharide-stabilized gold and silver nanoparticles: a green method. *Carbohydrate Research, 339*(15), 2627–2631.

Imberty, A., Chanzy, H., Perez, S., Buleon, A., & Tran, V. (1988). The double-helical nature of the crystalline part of A-starch. *Journal of Molecular Biology, 201*(2), 365–378.

Jenkins, P. J., & Donald, A. M. (1995). The influence of amylose on starch granule structure. *International Journal of Biological Macromolecules, 17*, 315–321.

Jodelet, A., Rigby, N. M., & Colquhoun, I. J. (1998). Separation and NMR structural characterisation of singly branched [α]-dextrins which differ in the location of the branch point. *Carbohydrate Research, 312*(3), 139–151.

Kaniyankandy, S., Nuwad, J., Thinaharan, C., Dey, G. K., & Pillai, C. G. S. (2007). Electrodeposition of silver nanodendrites. *Nanotechnology, 18*(12).

Li, L., & Zhu, Y.-J. (2006). High chemical reactivity of silver nanoparticles toward hydrochloric acid. *Journal of Colloid and Interface Science, 303*(2), 415–418.

Lu, L., Randjelovic, I., Capek, R., Gaponik, N., Yang, J., Zhang, H., & Eychmuller, A. (2005). Controlled fabrication of gold-coated 3D ordered colloidal crystal films and their application in surface-enhanced Raman spectroscopy. *Chemistry of Materials, 17*(23), 5731–5736.

Lu, Q., Gao, F., & Komarneni, S. (2005). A green chemical approach to the synthesis of Tellurium nanowires. *Langmuir, 21*(13), 6002–6005.

Moorthy, S. N., Andersson, L., Eliasson, A.-C., Santacruz, S., & Ruales, J. (2006). Determination of amylose content in different starches using modulated differential scanning calorimetry. *Starch - Stärke, 58*, 209–214.

Oates, C. G. (1990). Fine structure of mung bean starch: an improved method of fractionation. *Starch - Stärke, 42*, 464–467.

Panigrahi, S., Praharaj, S., Basu, S., Ghosh, S. K., Jana, S., Pande, S., Vo-Dinh, T., Jiang, H., & Pal, T. (2006). Self-assembly of silver nanoparticles: synthesis, stabilization, optical properties, and application in surface-enhanced Raman scattering. *Journal of Physical Chemistry B, 110*(27), 13436–13444.

Potiyaraj, P., Kumlangdudsana, P., & Dubas, S. T. (2007). Synthesis of silver chloride nanocrystal on silk fibers. *Materials Letters, 61*(11–12), 2464–2466.

Qu, L., Dai, L., & Osawa, E. (2006). Shape/size-controlled syntheses of metal nanoparticles for site-selective modification of carbon nanotubes. *Journal of the American Chemical Society, 128*(16), 5523–5532.

Raveendran, P., Fu, J., & Wallen, S. L. (2003). Completely "green" synthesis and stabilization of metal nanoparticles. *Journal of the American Chemical Society, 125*(46), 13940–13941.

Raveendran, P., Fu, J., & Wallen, S. L. (2006). A simple and green method for the synthesis of Au, Ag, and Au–Ag alloy nanoparticles. *Green Chemistry, 8*, 34–38.

Rindlav-Westling, A., Stading, M., & Gatenholm, P. (2002). Crystallinity and morphology in films of starch, amylose and amylopectin blends. *Biomacromolecules, 3*(1), 84–91.

Sarma, T. K., & Chattopadhyay, A. (2004). Starch-mediated shape-selective synthesis of Au nanoparticles with tunable longitudinal plasmon resonance. *Langmuir, 20*(9), 3520–3524.

Somsook, E., Hinsin, D., Buakhrong, P., Teanchai, R., Mophan, N., Pohmakotr, M., & Shiowatana, J. (2005). Interactions between iron(III) and sucrose, dextran, or starch in complexes. *Carbohydrate Polymers, 61*(3), 281–287.

Stoeva, S. I., Lee, J.-S., Thaxton, C. S., & Mirkin, C. A. (2006). Multiplexed DNA detection with biobarcoded nanoparticle probes. *Angewandte Chemie International Edition, 45*(20), 3303–3306.

Su, K. H., Wei, Q. H., Zhang, X., Mock, J. J., Smith, D. R., & Schultz, S. (2003). Interparticle coupling effects on plasmon resonances of nanogold particles. *Nano Letters, 3*(8), 1087–1090.

Sun, Y., & Xia, Y. (2002). *Shape-controlled synthesis of gold and silver nanoparticles Science, 298*, 2176–2179.

Tan, H. Z., Gu, W. Y., Zhou, J. P., Wu, W. G., & Xie, Y. L. (2006). Comparative study on the starch noodle structure of sweet potato and mung bean. *Journal of Food Science, 71*(8), C447–C455.

Templeton, A. C., Pietron, J. J., Murray, R. W., & Mulvaney, P. (2000). Solvent refractive index and core charge influences on the surface plasmon absorbance of alkanethiolate monolayer-protected gold clusters. *Journal of Physical Chemistry B, 104*(3), 564–570.

Tester, R. F., Karkalas, J., & Qi, X. (2004). Starch-composition, fine structure and architecture. *Journal of Cereal Science, 39*(2), 151–165.

Xu, Z. P., Hua Zeng, Q., Lu, G. Q., & Bing Yu, A. (2006). Inorganic nanoparticles as carriers for efficient cellular delivery. *Chemical Engineering Science, 61*(3), 1027–1040.